



**HAL**  
open science

## ptARgenOM-A Flexible Vector For CRISPR/CAS9 Nonviral Delivery

Abdelmnim Radoua, Baptiste Pernon, Nicolas Pernet, Chloé Jean,  
Mohammed Elmallah, Abderrahmane Guerrache, Andrei Alexandru  
Constantinescu, Sofiane Hadj Hamou, Jérôme Devy, Olivier Micheau

► **To cite this version:**

Abdelmnim Radoua, Baptiste Pernon, Nicolas Pernet, Chloé Jean, Mohammed Elmallah, et al..  
ptARgenOM-A Flexible Vector For CRISPR/CAS9 Nonviral Delivery. *Small Methods*, 2023, 7 (7),  
pp.e2300069. 10.1002/smt.202300069 . inserm-04138961

**HAL Id: inserm-04138961**

**<https://inserm.hal.science/inserm-04138961v1>**

Submitted on 23 Jun 2023

**HAL** is a multi-disciplinary open access archive for the deposit and dissemination of scientific research documents, whether they are published or not. The documents may come from teaching and research institutions in France or abroad, or from public or private research centers.

L'archive ouverte pluridisciplinaire **HAL**, est destinée au dépôt et à la diffusion de documents scientifiques de niveau recherche, publiés ou non, émanant des établissements d'enseignement et de recherche français ou étrangers, des laboratoires publics ou privés.



Distributed under a Creative Commons Attribution 4.0 International License

# ptARgenOM—A Flexible Vector For CRISPR/CAS9 Nonviral Delivery

Abdelmnim Radoua, Baptiste Pernon, Nicolas Pernet, Chloé Jean, Mohammed Elmallah, Abderrahmane Guerrache, Andrei Alexandru Constantinescu, Sofiane Hadj Hamou, Jérôme Devy, and Olivier Micheau\*

Viral-mediated delivery of the CRISPR-Cas9 system is one of the most commonly used techniques to modify the genome of a cell, with the aim of analyzing the function of the targeted gene product. While these approaches are rather straightforward for membrane-bound proteins, they can be laborious for intracellular proteins, given that selection of full knockout (KO) cells often requires the amplification of single-cell clones. Moreover, viral-mediated delivery systems, besides the Cas9 and gRNA, lead to the integration of unwanted genetic material, such as antibiotic resistance genes, introducing experimental biases. Here, an alternative non-viral delivery approach is presented for CRISPR/Cas9, allowing efficient and flexible selection of KO polyclonal cells. This all-in-one mammalian CRISPR-Cas9 expression vector, ptARgenOM, encodes the gRNA and the Cas9 linked to a ribosomal skipping peptide sequence followed by the enhanced green fluorescent protein and the puromycin N-acetyltransferase, allowing for transient, expression-dependent selection and enrichment of isogenic KO cells. After evaluation using more than 12 distinct targets in 6 cell lines, ptARgenOM is found to be efficient in producing KO cells, reducing the time required to obtain a polyclonal isogenic cell line by 4–6 folds. Altogether ptARgenOM provides a simple, fast, and cost-effective delivery tool for genome editing.

defense system,<sup>[1]</sup> whose nuclease, the Cas9, is being extensively used, in multiple organisms, to generate inheritable genetic alterations.<sup>[1,2]</sup> This gene editing method is the prevailing method in research laboratories to edit genes of interest.<sup>[2,3]</sup> While this approach is spreading, quickly replacing siRNAs or shRNAs, and despite the fact that it can be easily used and mastered to fully suppress any membrane-bound receptor or glycoprotein, its use for intracellular proteins can be cumbersome. Lenti- or retroviral systems to deliver the CRISPR/Cas9 and gRNA of interest, are increasingly being used, but these approaches are not affordable to most laboratories worldwide, due to a lack of dedicated space equipment, including a biosafety level-2 culture room and high maintenance costs. Furthermore, bearing in mind that these viral delivery systems have a propensity for random integration into the host cell genome, leading to constitutive expression of selection genes (fluorescent or

antibiotic resistance), as well as gRNA and Cas9, they are likely to introduce bias in the study and lead to erroneous conclusions, especially when clones are concerned.<sup>[4]</sup> Alternative systems based on recombinant Cas9 and RNPs<sup>[5]</sup> are also available commercially, and much less likely to introduce bias. Yet, these

## 1. Introduction

Gene editing is widely used nowadays to study protein function. The Clustered Regularly Interspaced Short Palindromic Repeats CRISPR/Cas9 system is a naturally occurring anti-viral bacterial

A. Radoua, B. Pernon, N. Pernet, M. Elmallah, A. Guerrache, A. A. Constantinescu, S. Hadj Hamou, O. Micheau  
UFR des Sciences de Santé  
Université de Bourgogne  
Dijon 21000, France

A. Radoua, N. Pernet, A. Guerrache, O. Micheau  
INSERM  
Université de Bourgogne Franche-Comté (UBFC), UMR1231, LNC  
Dijon 21000, France  
E-mail: omicheau@u-bourgogne.fr

C. Jean, J. Devy  
UFR Sciences Exactes et Naturelles  
Université de Reims Champagne-Ardenne (URCA)  
Reims, Cedex 51687, France

C. Jean, J. Devy  
Matrice Extracellulaire et Dynamique Cellulaire  
MEDyC  
UMR 7369 CNRS, Reims 51687, France

M. Elmallah  
Chemistry Department  
Faculty of Science  
Helwan University  
Ain Helwan, Cairo 11795, Egypt

 The ORCID identification number(s) for the author(s) of this article can be found under <https://doi.org/10.1002/smt.d.202300069>

© 2023 The Authors. Small Methods published by Wiley-VCH GmbH. This is an open access article under the terms of the Creative Commons Attribution License, which permits use, distribution and reproduction in any medium, provided the original work is properly cited.

DOI: 10.1002/smt.d.202300069

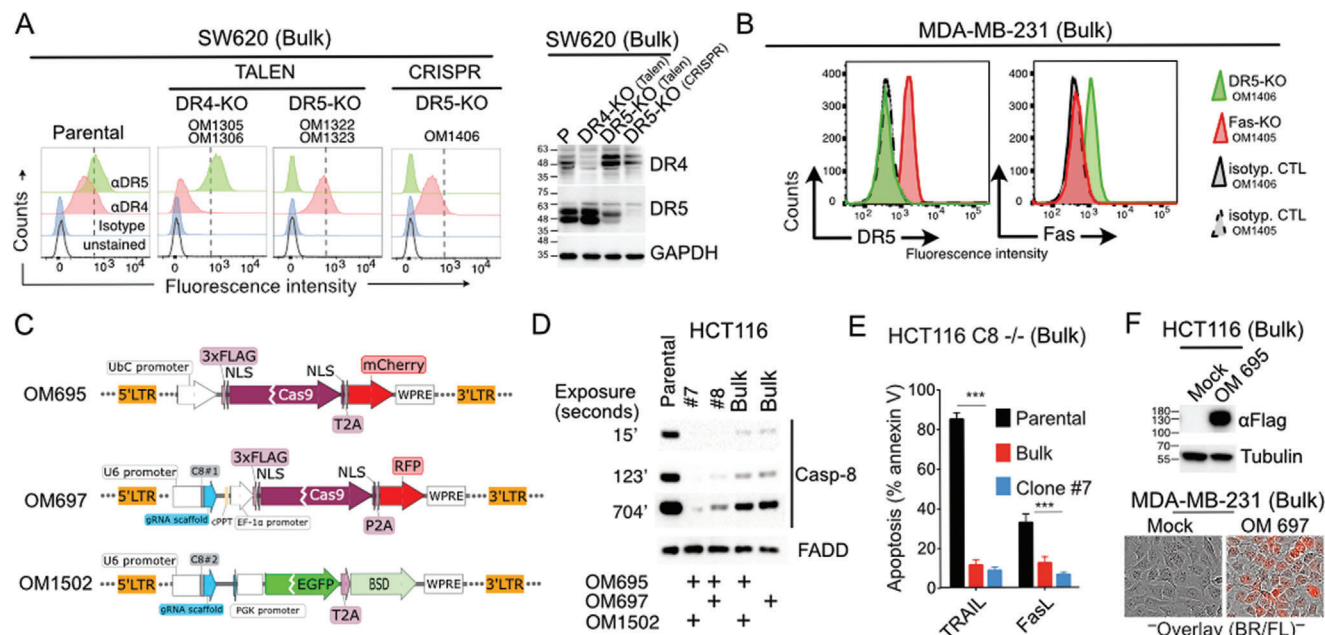


**Figure 1.** Generation of gene edited bulk cells is straightforward for transmembrane proteins but much more difficult for intracellular proteins. A) Flow cytometry and immunoblot analysis of DR4 or DR5 expression in SW620 parental cells compared to SW620 DR4- or DR5-deficient polyclonal cells generated either by transfection with the TALEN or by infection with the CRISPR/Cas9 approaches. GAPDH served here as a loading control. B) Flow cytometry analysis of DR5 or Fas expression in MDA-MB-231 DR5- or Fas-deficient cells obtained by CRISPR/Cas9. Isotype controls are shown as filled grey histograms. DR5 and Fas are shown in green and red, respectively. C) Illustration of the retroviral vector used to express the Cas9 and knock-out the caspase-8 in HCT116 cells. D) Immunoblots showing cell polyclonal cells (Bulk) or derivative clones (#7 and #8) edited for the caspase-8 using one or two distinct caspase-8 gRNAs. FADD served here as a loading control. Exposure time is shown in seconds. E) Cell sensitivity of the corresponding caspase-8-deficient HCT116 cells or the derivative clone #7 to TRAIL- or Fas ligand-induced cell death measured by flow cytometry using annexin-V staining. F) Immunoblot of the HCT116 caspase-8 KO cells generated with the lentiviral vector OM697, with indicated antibodies, expressing constitutively the Cas9. Tubulin served here as a loading control. Below are shown the phase contrast and fluorescence overlay of MDA-MB-231 infected with the lentiviral vector OM 697 compared to mock infected cells.

systems are expensive and, with the exception of T cells, for which deficient bulk polyclonal cells have been described for membrane-bound proteins,<sup>[6,7]</sup> to the best of our knowledge, no simple and affordable gene-editing system has been described for its convenience and ease of use in generating bulk polyclonal cells deficient for an intracellular protein of interest.

Thus, to avoid bias generated by the use of CRISPR/Cas9 viral-based vector systems, and in order to reduce the time needed to select KO bulk polyclonal cells, we have designed a bi-modal plasmid vector encoding both the Cas9 and the gRNA of interest as well as the enhanced green fluorescent protein (EGFP) and the puromycin resistance gene, for fast selection of transiently transfected polyclonal cells deficient for the given gene of interest. Our vector, coined ptARgenOM, allows in a cost-effective and flexible manner, fast generation of fully knock-out cells, including hard to delete or abundant intracellular gene products.

## 2. Results

### 2.1. Viral CRISPR/Cas9 Delivery Is Efficient in Generating Membrane-Bound-Target Deficient Polyclonal Cells but Less So for Intracellular Proteins

With the exception of transmembrane proteins, which allow negative cell sorting,<sup>[8,9]</sup> the generation of polyclonal cells deficient for intracellular proteins is not common. Rather, and regardless

of the technique used, TALEN or CRISPR/Cas9, gene deletion is most often achieved through isolation and selection of single-cell clones.<sup>[10]</sup> Only a limited number of publications have, so far, described the generation of polyclonal gene-edited cells,<sup>[9,11,12]</sup> but none of these have obtained full knockout (KO). Likewise, while generation of complete KO is easily achieved for transmembrane proteins, as exemplified here with the TALEN or CRISPR/Cas9 approaches on DR4, DR5, and Fas receptors (Figure 1A,B), the complete KO of intracellular proteins, such as the caspase-8 can be difficult to achieve, regardless of the guide RNA or methodological approach used, including flow cytometry-based sorting of cells infected with lentiviruses allowing expression of EGFP, mCherry or RFP and Cas9 (Figure 1C,D). Indeed, despite the fact that these polyclonal isogenic cell lines show reduced caspase-8 expression levels (Figure 1D) and reduced sensitivity to both Fas ligand- or TRAIL-induced cell death (Figure 1E), as expected, a fraction of the polyclonal cells, albeit small, still expresses the caspase-8 (Figure 1D). Moreover, these viral delivery systems, besides allowing editing of the locus of interest, permanently modify the host isogenic cells by integrating their genetic material into the host genome. Likewise, the lentiviral CRISPR/CAS9 system, used here to edit the caspase-8 in the colorectal cancer cell line HCT116, led to the integration of both the Cas9 as well as to the Red Fluorescent protein cDNA sequences in MDA-MB-231 cells, as demonstrated by immunoblot and immunofluorescence (Figure 1F).

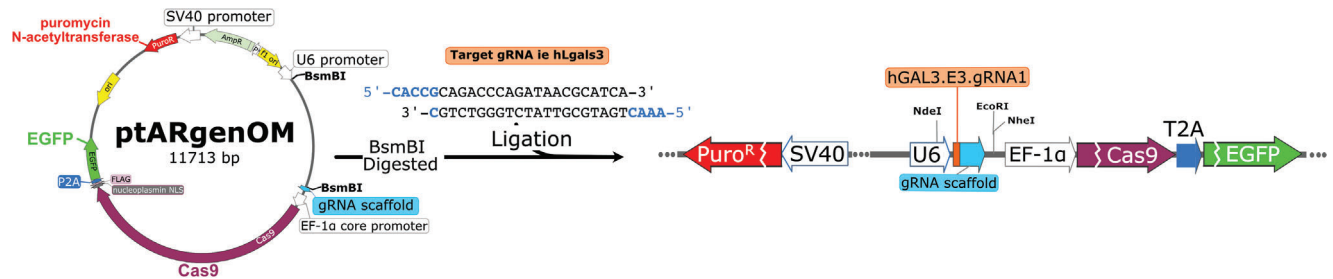


Figure 2. Schematic illustration of ptARgenOM.

## 2.2. Nonviral CRISPR/Cas9 Delivery Allows Efficient Generation of Intracellular Protein Targets Knockout Clones

To avoid the integration of unwanted genetic material in the host genome, including the delivery CRISPR/Cas9 DNA system selection genes, we have designed an all-in-one pCR3-based transient eucaryotic delivery vector system (see Table S1, Supporting Information). Our vector, coined ptARgenOM (Figure 2), harbors a BsmBI gRNA cloning site downstream the U6 promoter and encodes the Cas9 fused to a ribosomal skipping peptide sequence (P2A) and the EGFP as well as the puromycin N-acetyltransferase, which confers cell resistance to the antibiotic puromycin, allowing transient selection of transfected cells (Figure 2). Much like the reference lentiviral vector, pLentiCRISPR v2,<sup>[13,14]</sup> ptARgenOM allows easy cloning of gRNAs as shown Figure 2 using the restriction enzyme BsmBI. Unlike the lenti- or retroviral-systems, however, ptARgenOM is devoid of LTRs and thus is far less likely to get integrated into the host genome.

As a proof-of-concept and in order to assess the gene editing potential of ptARgenOM, in particular for genes encoding intracellular proteins, we set up an experiment with 3 distinct validated gRNAs targeting either *C1GALT1C1* (COSMC) and *MGAT1*<sup>[15]</sup> or *LGALS3*.<sup>[16]</sup> Targeted loci are shown in Figure S1 (Supporting Information). After transfection, viable cells (FVS660 negative) were sorted as single cells, based on the expression of the EGFP, and allowed to grow for 6 to 8 weeks (Figure 3A), before analyzing the loss of protein expression by immunoblot or flow cytometry. Clone nomenclature, as indicated Figure 3A, consisted of the initial of the targeted gene product followed by the coordinates of the 96 well plate in which the clone was found. For both colorectal cancer cell lines, HCT116 and SW620, analysis of the loss of expression of COSMC, MGAT1 and Galectin-3 or expression levels of O- and N-glycosylated proteins, using the lectins PHA and VVL,<sup>[15]</sup> indicating that the ptARgenOM allowed the generation of gene-deficient cell clones (Figure 3). The loss of COSMC and MGAT1 protein expression was clearly evidenced in positive clones by immunoblot (Figure 3B,D) and flow cytometry (Figure 3C,E). Likewise, the loss of N-linked glycosylation in MGAT1-KO cell clones was associated with a lack of expression of MGAT1 (Figure 3B,D) and the loss of PHA staining in both cell lines (Figure 3C,E). Noteworthy, as expected,<sup>[17]</sup> impaired N-glycosylation was also associated with an increased electrophoretic mobility of DR4 in HCT116 (Figure 3B,D), slight reduction of DR4 staining, but not DR5, as assessed by flow cytometry (Figure 3C,E and Figure S2A, Supporting Information) and, in agreement with pre-

vious finding,<sup>[17]</sup> reduced TRAIL-apoptotic signaling activity as shown by fluorescence microscopy and flow cytometry (Figure S2B,C, Supporting Information). Moreover, and consistent with the putative N-glycosylation sites harbored by TNFR1,<sup>[18–20]</sup> loss of N-glycosylation induced in MGAT1-/- cells, albeit to a lesser extent as compared to DR4, was associated with faster electrophoretic mobility of TNFR1 (Figure 3B). Loss of O-linked glycosylation in COSMC-KO cell clones, on the other hand, was much more difficult to detect with the anti-COSMC antibody used herein, but could be objectivated by immunoblot, nevertheless, by the disappearance of the lower band (Figure 3B,D). This is consistent with the increase in VVL staining, as detected by flow cytometry,<sup>[15]</sup> in COSMC-deficient clones (Figure 3C,E), or the loss of sensitivity of these cell clones to TRAIL-induced cell death (Figure S2B,C, Supporting Information), as described previously by Wagner et al.<sup>[21]</sup> O-link-deficiency was also associated with an increased electrophoretic mobility of a fraction of the MGAT1 proteins (Figure 3B,D). MGAT1 is thus likely to undergo post-translational modifications of the oglycosylation type, given that MGAT1 harbors 4 putative O-glycosylation sites (T51, T88, T100 and S320; www.glygen.org/protein/P26572). Loss of O-glycosylation of MGAT1, however, did not appear to inhibit MGAT1's activity, since COSMC-KO cells display proper N-glycosylation, as shown by lectin PHA staining (Figure 3C,E). Similar to MGAT1, loss of galectin-3 was easily evidenced by immunoblot (Figure 3D). The deletion efficiency in these cells was calculated relatively to the total number of clones analyzed. With 7 and 12 clones fully deficient out of 11 and 20 HCT116 and SW620 cell clones, respectively, the efficiency reached 60 to 63% (Figure 3F). The CRISPR/Cas9 ptARgenOM vector, in addition to the EGFP, also encodes a puromycin N-acetyltransferase, which can also serve, after transfection, for selecting KO cell clones or polyclonal cells using puromycin (Figure 3G). Because the puromycin resistance gene is under the control of the SV40 promoter, we first tested whether ptARgenOM could be used in HEK293T cells, which express the large T antigen, to generate COSMC and MGAT1 KO cell line clones, after transient puromycin selection (Figure 3G). Again, like cell clones sorted by flow cytometry based on their expression level of the EGFP, selection with puromycin was found to be efficient since 6 clones out of 10 displayed a deficiency for the targeted gene product as analyzed by immunoblot (Figure 3H,I). Of note, unlike lentiviral or retroviral systems, the KO clones obtained using ptARgenOM, albeit selectable based on the transient expression of both the EGFP and the puromycin N-acetyltransferase, for their vast majority, do not integrate these selection markers in their genome.

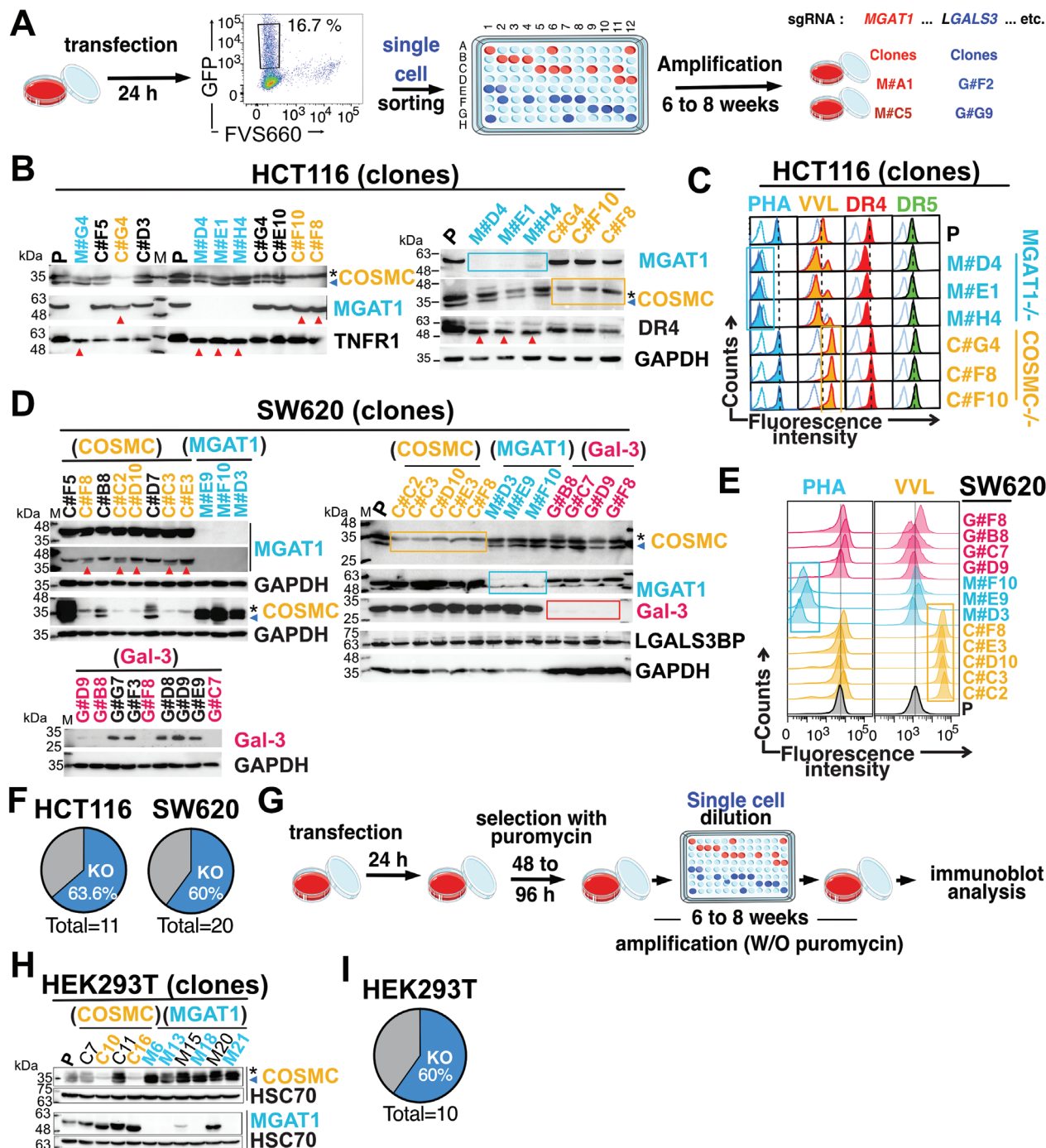


**Figure 3.** Generation of KO single clones using ptARgenOM. A) Illustration of the protocol used to generate deficient clones after single cell sorting. After seeding, cells were transiently transfected with indicated ptARgenOM.sgRNAs (*COSMC*, *MGAT1* or *LGALS3*) and allowed to express the EGFP for 24h. Viable (FVS660 negative) EGFP positive cells were next sorted individually in a 96-well plate. Clones were allowed to grow for 6 to 8 weeks and analyzed by immunoblot. Clone nomenclature systematically associates the first letter the targeted gene followed by # and its position in the 96-well plate. For example, M#A1 & M#C5 corresponds to two distinct *MGAT1* KO clones grown in position A1 and C5, respectively. B) Immunoblot of HCT116 parental (P) or *MGAT1*<sup>-/-</sup> and *COSMC*<sup>-/-</sup> clones and C) flow cytometry analysis of the corresponding clones labelled with anti-DR4, and -DR5 antibodies or PHA- and VVL-lectins. D) Immunoblots of SW620 *MGAT1*<sup>-/-</sup>, *COSMC*<sup>-/-</sup> and Gal-3<sup>-/-</sup> clones. E) Flow cytometry analysis of SW620 parental (P) or *MGAT1*<sup>-/-</sup>, *COSMC*<sup>-/-</sup> and Gal-3<sup>-/-</sup> clones with the indicated lectins. F) Pie chart representation of the knock-out (KO) efficacy in HCT116 and SW620 cells. G) Illustration of the protocol used to generate deficient clones after single cell dilution and puromycin selection. HEK293T cells were transfected as above and treated 24 h after transfection with puromycin for 48 to 96 h before limiting dilution and seeding of single cells into a 96-well plate. Viable single-cell clones were then amplified for 6 to 8 weeks. H) Immunoblot analysis of corresponding *COSMC*<sup>-/-</sup> and *MGAT1*<sup>-/-</sup> HEK293T clones. I) Pie chart representation of the knock-out efficacy in HEK293T cells. In this figure the red triangle indicates an electrophoretic mobility change of a protein. The star \* indicates the non-specific *COSMC* immunolabeling. The blue triangle shows *COSMC* specific staining.

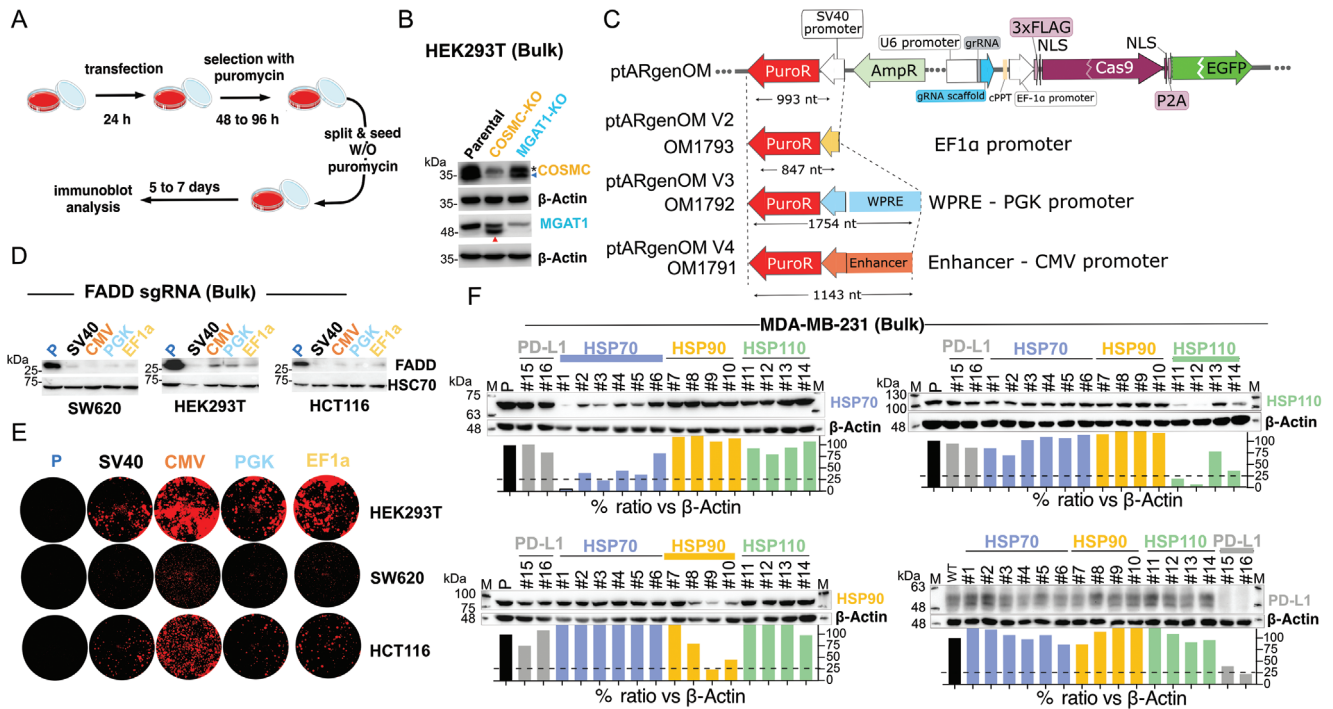


**Figure 4.** Generation of KO polyclonal deficient cells using ptARgenOM.sgRNAs and puromycin selection. A) Illustration of the protocol used to generate bulk deficient KO-cells. After seeding, cells were transfected as indicated Figure 3 with distinct ptARgenOM.sgRNAs (COSMC, MGAT1), treated for 48 to 96 h with puromycin, and polyclonal cells (Bulk) were allowed to grow for 5 to 7 d before analysis by immunoblot. B) Immunoblot analysis of corresponding HEK293T parental or KO-cells. C) Illustration of the different versions of ptARgenOM in which the SV40 puromycin promoter was replaced by the EF1 $\alpha$ , PGK or CMV promoters. D) Immunoblot analysis of FADD expression after transfection of the indicated cell lines with corresponding ptARgenOM versions encoding a FADD sgRNA, as compared to parental cells. HSC70 was used as a loading control. E) Artificial image analysis generated with Incucyte S3, showing cell density after transfection with ptARgenOM versions and puromycin selection (72 h). F) Immunoblot analysis of HSP70, HSP90, HSP110, and PD-L1 KO after one round of transfection using ptARgenOM.sgRNAs (#1 to #16; from 2 to 6 sgRNAs per gene targeted). Actin was used as a loading control. Below are shown the semi-quantitative analysis of the corresponding immunoblots performed using the free ImageJ Fiji software (National Institutes of Health, Bethesda, MD). In this figure, the red triangle indicates an electrophoretic mobility change of a protein. The star \* indicates the nonspecific COSMC immunolabeling. The blue triangle shows COSMC specific staining.

Likewise, and as estimated by rechallengeg EGFP selected deficient cells to puromycin treatment, two weeks to 5 months after transfection, these cells remained sensitive to puromycin and did not express the EGFP anymore (not shown).

To corroborate the loss of protein expression of some of these clones (Figure S3A, Supporting Information) with the genomic modifications induced by the gRNAs and Cas9 transient expression, we designed primers, encompassing or included in the targeted locus (Figures S3B, Supporting Information), to detect by PCR the presence, the absence or changes of expected products within the given loci (Figure S3C, Supporting Information). Of the 6 distinct clones analyzed, 3 displayed obvious alterations at the genomic level when one of the amplifying primers (P2 or P3) was located within the targeted locus (Figure S3C, Supporting Information). Likewise, no PCR product could be generated in COSMC-deficient HCT116 cell clone C#C2 as opposed to parental or clone C#D10 with COSMSC primers P1 and P2. Similarly, no PCR products were generated using GAL3 primers P3 and P4 for clone G#C7, whereas in clone G#B8 less PCR products were obtained as compared to parental cells (Figure S3C, Supporting Information). On the other hand, using primers encompassing the targeted locus (P1 and P4), we observed a larger PCR product, in the G#B8 clone (Figure S3C, Supporting Infor-

mation). This insertion of approximately 250 nt was analyzed, after TA cloning and sequencing, and found to correspond to the C-terminal portion of the EGFP, corresponding to the nucleotide sequence 366 to 611 of EGFP ORF (aa122 to 203), and originating from ptARgenOM (Figure S3D, Supporting Information). Sequencing the PCR products obtained from other clones showed that most of the genomic alterations, however, corresponded to either substitutions and/or deletions, as expected.

### 2.3. Generation of Bulk Polyclonal Isogenic KO Cells Using ptARgenOM

We next evaluated whether ptARgenOM would allow us to generate KO bulk polyclonal cells after selection of the transfected cells with puromycin (Figure 4A). Because the puromycin resistance gene is under the control of the SV40 promoter, we first tested whether ptARgenOM could be used in HEK293T cells to generate COSMC and MGAT1 KO polyclonal cells (Figure 4A). Although the knock-down of COSMC or MGAT1 was evident, 7 days after transfection in these cells (Figure 4B), full MGAT1 or COSMC KO was not achieved after a single round of transfection (Figure 4B). Replacing the SV40 promoter by the EF1 $\alpha$ , CMV or

the PGK promoter (Figure 4C), as tested with a sgRNA targeting *FADD*, an essential adaptor protein of the TNF superfamily, did not increase the efficacy of ptARgenOM, in generating full KO in SW620, HEK293T or HCT116 cells as assessed by immunoblot (Figure 4D). However, some of them, such as the CMV promoter, allowed faster recovery of the polyclonal cells after transfection (Figure 4E), due most probably to earlier and stronger expression of the puromycin N-acetyltransferase. Regardless of the promoter, ptARgenOM was found to be particularly useful for the selection of gRNAs of interest after puromycin selection. Likewise, and as illustrated Figure 4F with the immunoblots of MDA-MB-231 cells transfected with gRNAs targeting HSP70, HSP90, HSP110, ptARgenOM allowed the screening of efficient gRNAs in less than 2 weeks. Similar to HSP targets, ptARgenOM allowed us to produce PD-L1-deficient cells, after short-term puromycin selection, as demonstrated by immunoblot (Figure 4F) and flow cytometry (Figure S4A, Supporting Information). The selection of 2 to 6 gRNAs per target, using CRISPOR,<sup>[22]</sup> was sufficient to identify gRNAs targeting specifically HSP70, HSP90, HSP110, and PD-L1 in our cells (Figure 4F).

Whereas bulk puromycin selection was sufficient to screen the most appropriate sgRNAs, depending on the target gene, this was not sufficient, with a single round of transfection, to generate full KO isogenic polyclonal cells. We reasoned that selecting cells expressing high level of EGFP and thus high levels of Cas9 would likely increase edition events in the selected cells, and thus favor enrichment of gene-edited cells. In agreement with this hypothesis, cell sorting of ptARgenOM transiently transfected cells for low, medium or high levels of EGFP expression (Figure 5A), clearly demonstrated, that the more EGFP/Cas9 was expressed, the more the genome was edited, as illustrated by the loss of protein expression of MGAT1 and Galectin-3 (Figure 5B). Loss of COSMC expression after edition, as indicated earlier, was not easily detected by immunoblot using our anti-COSMC antibody (Figure 5B), but was clearly evidenced by the increase of electrophoretic mobility of a fraction of MGAT1 (Figure 5B) as well as by the high expression of VVL by flow cytometry (see for example Figure S7C, Supporting Information). Selecting cells expressing the highest EGFP expression levels after transfection with ptARgenOM enabled the generation of polyclonal cells displaying almost complete gene edition (Figure 5C,D). Given that the whole procedure can be achieved within two weeks, we tested whether a second round of transient transfection and cell sorting would allow enrichment and selection of KO cells fully deficient for the protein of interest. Using a gRNA targeting the adaptor protein *FADD* we demonstrate here that generation of bulk fully deficient cells can be achieved with ptARgenOM in less than one month after two rounds of transfection (Figure 5E,F).

The versatility of ptARgenOM for selecting gRNAs of interest and generating fully deficient cells the corresponding target, was further challenged by comparing side-by-side the efficacy of the vector in generating cells deficient for COSMC, MGAT1 or Gal-3 in MDA-MB231 cells after puromycin selection versus high-EGFP cell sorting. Results shown Figure S4 (Supporting Information) clearly indicate that both approaches can be used in a somewhat similar fashion to generate cells deficient for the protein of interest (Figure S4A,B, Supporting Information). Again, illustrating the flexibility of ptARgenOM and regardless of whether KO cells were selected with puromycin or af-

ter cell sorting, our vector allowed fast identification of efficient LRP-1 gRNAs (Figure S4C, Supporting Information). Noteworthy, ptARgenOM enabled the generation of bulk polyclonal cells deficient for LRP-1, in both the human and mice tumor cell lines BT-20 and 4T1, respectively (Figure S4C, Supporting Information). Moreover, sequential selection with puromycin and sorting of high-EGFP expressing cells after two rounds of transfections, as illustrated Figure S4D (Supporting Information), yielded substantial enrichment of bulk knockout cells. Likewise, albeit full KO was not reached with the *IgalS3* gRNA, this sequential transfection approach consistently reduced each time the amount of both *FADD* and *galectin3* expressed in the transfected cells, and full deficiency was obtained using the *FADD* gRNA (Figure S4E, Supporting Information). Regardless of *galectin-3* gRNA's efficacy, our results, altogether, clearly indicate that ptARgenOM is a potent and flexible CRISPR/cas9 delivery vector that allows production of isogenic KO polyclonal cells.

#### 2.4. Functional Validation of Isogenic KO Polyclonal Cells Generated with ptARgenOM

In order to functionally validate the polyclonal cells generated using ptARgenOM, either after a one or two rounds of transfection followed by cell sorting of the highest EGFP expressing cells, we generated *FADD*<sup>-/-</sup>, *caspase-8*<sup>-/-</sup> and *RIPK1*<sup>-/-</sup> HCT116, MDA-MB-231 or SW620 cells. The expression levels of the corresponding targeted gene products were checked by immunoblot (Figure 6A). Regardless of the cell line, *FADD*<sup>-/-</sup> cells, that have undergone two rounds of transfections with ptARgenOM-*FADD*-gRNA, displayed complete deletion of *FADD* (Figure 6A) and were, as expected,<sup>[23,24]</sup> fully resistant to both TRAIL or Fas ligand (FasL) induced cell death, as demonstrated by Annexin-V and PI staining (Figure 6B,C). Noteworthy, with the exception of MDA-MB-231 cells, *FADD*<sup>-/-</sup> polyclonal cells, like all KO polyclonal cells generated with ptARgenOM are sensitive to puromycin (Figure S5, Supporting Information) and do not express the EGFP, as illustrated Figure 6C and Figure S6 (Supporting Information), clearly indicating that *FADD*<sup>-/-</sup> cells have not integrated foreign DNA originating from ptARgenOM. Single round of transfections, on the other hand, albeit less efficient in generating KO cells, as compared to the two rounds of transfections of *FADD* gRNA, led to at least 75% loss of *RIPK1* and *caspase8* expression in the three distinct adherent cell lines (Figure 6A) and behaved as expected in response to both FasL and TRAIL.<sup>[25,26]</sup> Likewise, whereas deletion of *caspase-8* inhibited apoptosis induced by TRAIL (Figure 6B,C), as efficiently as in the TRAIL-receptor-deficient cells (DKO),<sup>[8]</sup> deletion of *RIPK1*, as expected,<sup>[25]</sup> failed to impair apoptosis induced by either TRAIL, or FasL (Figure 6B,C). Quantitative analysis by flow cytometry, as well as qualitative analysis of apoptosis induced by TRAIL or FasL in these isogenic cell lines deleted for *FADD*, *caspase-8* or *RIPK1* (Figure 7A), clearly demonstrated that the polyclonal cells generated using ptARgenOM, are reliable and can ultimately be considered as KO cells for the given genes-of-interest, as targeted by our vector. Likewise, similar to TRAIL-receptor deficient cells (DKO), cells deficient for *FADD* and *caspase-8* are all significantly protected against apoptosis induced by TRAIL, as monitored by flow cytometry using Annexin-V and 7AAD staining (Figure 7A).

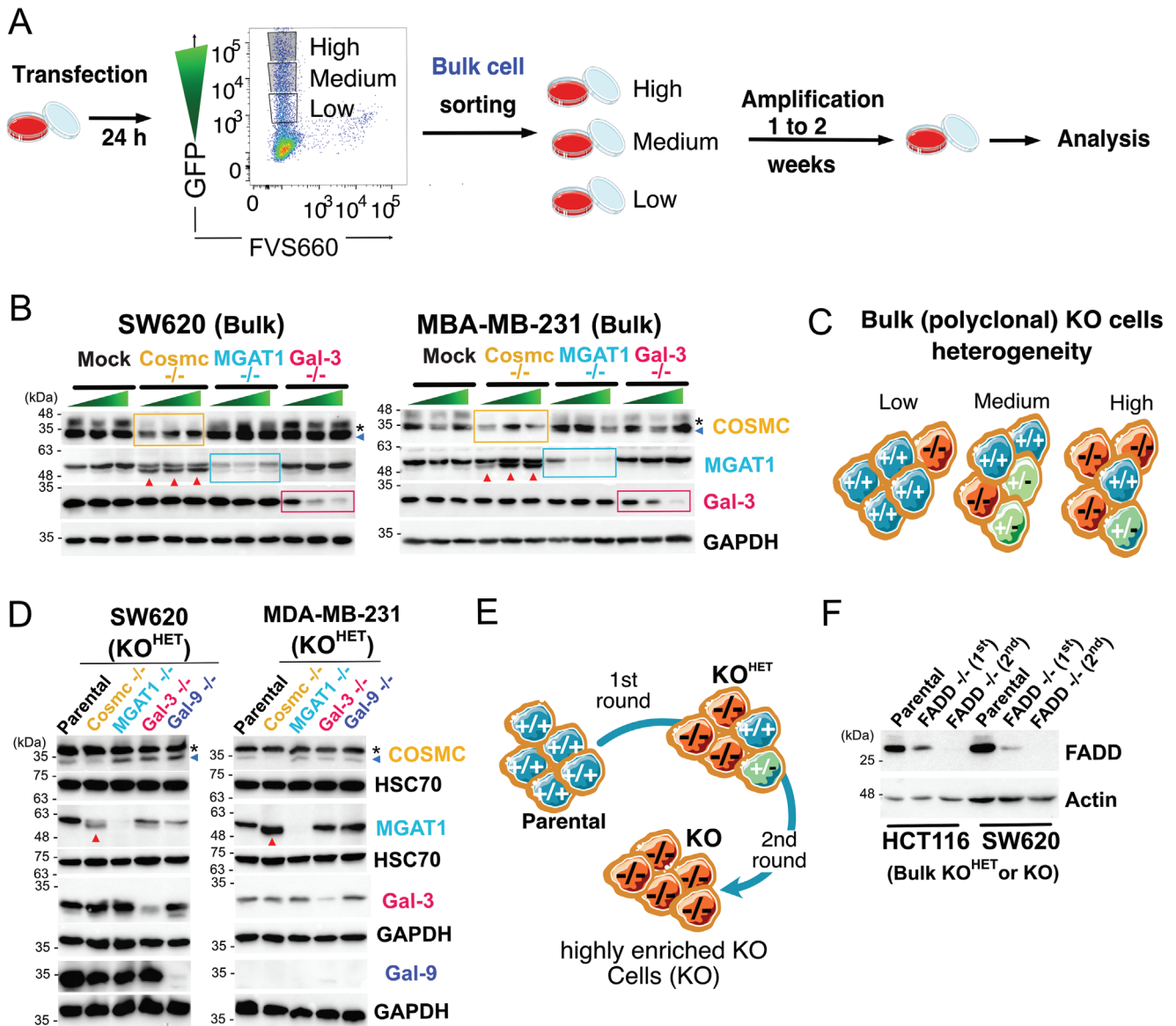


**Figure 5.** Generation of bulk KO cells using ptArgenOM.sgRNAs using flow cytometry and cell sorting. A) Illustration of the protocol used to generate bulk deficient KO-cells. After seeding, cells were transfected with distinct ptArgenOM.sgRNAs (COSMC, MGAT1, LGALS3 or LGALS9) and allowed to express the EGFP for 24h. Viable (FVS660 negative) EGFP positive cells were next sorted as pooled polyclonal cells (bulk,  $>5 \times 10^3$  cells) based on the intensity of the EGFP signal, low, medium and high. Cells were allowed to grow for 1 to 2 weeks before analysis by immunoblot. B) Immunoblot analysis of corresponding MDA-MB-231 and SW620 parental or KO-cells. C) Schematic illustration of the heterogeneity of the KO cells within the bulk population ( $KO^{HET}$ ), generated after transient transfection with ptArgenOM and flow cytometry-based cell sorting of low, medium or high EGFP expressing cells. D) Immunoblot analysis of MDA-MB-231 and SW620 parental (P) or  $KO^{HET}$  cells generated after EGFP<sup>high</sup> sorting. E) Illustration of the 2 rounds enrichment strategy used to generate homogeneous full deficient KO cells. F) Immunoblot analysis of FADD expression in HCT116 and SW620 FADD<sup>-/-</sup> cells after 1 and 2 rounds of transfections and bulk cell enrichment by flow cytometry. In this figure the red triangle indicates an electrophoretic mobility change of a protein. The star \* indicates the non-specific COSMC immunolabeling. The blue triangle shows COSMC specific staining.

In line with the lack of apoptosis induced by TRAIL in FADD<sup>-/-</sup> and caspase-8<sup>-/-</sup> cells, is the lack of activation of the effector caspase-3 and cleavage of its substrates, in corresponding protein extracts, as evidenced by immunoblot. Likewise, the appearance of their cleaved products was almost absent in these isogenic cells, as opposed to parental or RIPK1<sup>-/-</sup> cells that undergo extensive apoptosis and in which activation of the caspase-3 was

strongly induced both by TRAIL (Figure 7B). Similar results were obtained with FasL in these cells, except in TRAIL-deficient cells that display similar sensitivity to FasL as parental cells, as expected (Figure 7B). Effector caspase activation was in all cases tightly associated with the cleavage of the initiator caspases, including in MDA-MB-231 caspase-8<sup>-/-</sup> cells, in which residual levels of caspase-8 remains.

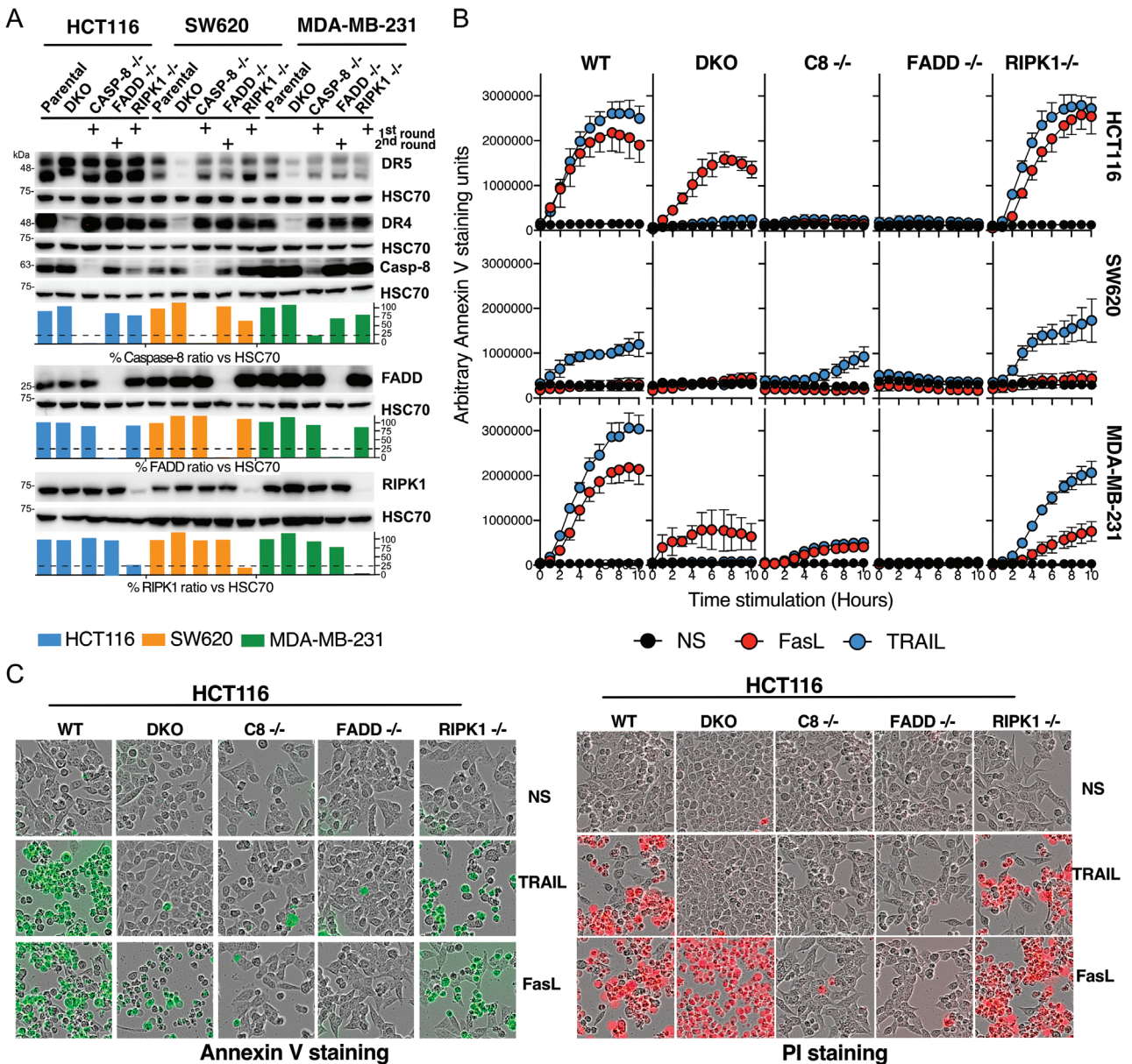


**Figure 6.** Validation of FADD-, Caspase-8-, and RIPK1-KO polyclonal cells by immunoblot and live cell imaging. A) Three distinct cell lines transfected either one time or twice with ptARgenOM.sgRNAs (FADD, caspase-8 or RIPK1) were analyzed by immunoblot for the indicated proteins, and compared to parental cells or DR4-/- and DR5-/- (DKO) cells. Histograms below corresponding immunoblots correspond to semi-quantitative protein expression levels quantified relative to the HSC70 staining from the same immunoblot membrane. B) IncuCyte S3 imager-based quantification of apoptosis (FITC Annexin-V staining) after TRAIL or Fas ligand stimulation of the indicated cell lines and deficient bulk isogenic cells. C) Representative IncuCyte images of annexin-V or PI staining 8 h after stimulation.

### 3. Discussion and Conclusion

The CRISPR-Cas9 system holds promises to permanently cure inherited genetic diseases.<sup>[27]</sup> Several clinical trials are assessing the potential application of this gene editing system in Duchenne muscular dystrophy,<sup>[28]</sup>  $\beta$ -thalassemia,<sup>[29]</sup> inherited retinal diseases,<sup>[30]</sup> sickle cell disease<sup>[31,32]</sup> or cancers.<sup>[33–35]</sup> In most cases, efficient delivery of the gene editing system, which is considered as a bottleneck, is achieved in hematopoietic cells or hematopoietic stem cells, including CAR-T cells, either using

viral-derived delivery systems or preassembled RNP complexes. Likewise, PD-1, TCR or CD33 in CAR-T cells are most often targeted using lentiviruses, adenoviruses<sup>[36]</sup> or preassembled RNP complexes.<sup>[37,38]</sup> Alternatively, the delivery may also be achieved, like in Duchenne's muscular dystrophy or  $\beta$ -thalassemia, using self-complementary AAV (scAAV) adeno-associated viruses or in vitro synthesized mRNAs.<sup>[29,35]</sup>

With the exception of mRNAs and RNP complexes, the safety of viral-mediated CRISPR/Cas9 delivery systems is questionable for clinical use.



of both N- and O-glycosylation in regulating apoptosis-induced by TRAIL.<sup>[17,21,46]</sup>

Another advantage of the bi-modal ptARgenOM vector, that we present here, besides its flexibility which allows bulk cell enrichment either or both through puromycin treatment or GFP-based cell sorting, is its efficacy in inducing gene edition, as demonstrated by immunostainings or sequencing analysis (Figures S7 and S8, Supporting Information), ranging from 60 to 90% after one round of transfection to more than 99.5% after two rounds of enrichment. The ease of use of ptARgenOM, and the possibility to enrich target gene-edited cells both by flow cytometry, based on the EGFP expression, or by using the puromycin, in a transient manner, allows for fast generation of homogeneous KO cells. Compared to conventional clonal KO cells, which, depending on the growth rate of the targeted cell line, require at least 9 to 12 weeks, ptARgenOM allowed the generation of KO polyclonal cells in less than 3 weeks, reducing the required generation time by 4 to 6-fold.

Altogether, ptARgenOM is a flexible gene-editing vector that allows fast and efficient generation of polyclonal knockout cells. We believe that this non-viral vector will be a valuable tool for the scientific community.

## 4. Experimental Section

**Plasmids and gRNA Cloning:** The plasmid vectors used in this study are described in Table S1 (Supporting Information). The ptARgenOM vectors were generated using the In-Fusion HD system.<sup>[47]</sup> Briefly, the main components of ptARgenOM, including the Cas9, EGFP, the puromycin N-acetyltransferase or the promoters of interest were amplified by PCR using the PrimeSTAR Max DNA Polymerase (Takara), as described in detail in Tables S2 and S3 (Supporting Information). The primers are described in Table S4 (Supporting Information). PCR products were extracted and assembled using the In-Fusion HD Cloning kit (Takara) as recommended by the provider and transformed in Stellar competent cells (Takara). All gRNAs were designed using the online tools <http://crispor.tefor.net/><sup>[22]</sup> and <https://sgnascorer.cancer.gov/dbguide/>.<sup>[48]</sup> The oligonucleotides were designed and cloned as described previously.<sup>[13,14]</sup> The ACPR30-FasL cDNA,<sup>[49]</sup> kind gift from Pr Pascal Schneider (Department of Immunobiology, University of Lausanne, Epalinges, Switzerland) was cloned into the lentiviral vector pAIP (Addgene # 74171). The TRAIL-Mu3 coding sequence, based on the information published previously by Zhu et al.,<sup>[50]</sup> was obtained from Genscript and cloned into a modified version of pET100D, as described by Shilling et al.<sup>[51,52]</sup>

**TA Cloning and Sequencing:** Genomic DNA was extracted from cells using PureLink Genomic DNA mini kit (ThermoFisher, K182002) according to manufacturer's recommendation. Loci of interest were amplified using specific oligonucleotides flanking the gRNA target sequence (Table S4, Supporting Information). The oligonucleotides were designed using Primer-blast on NCBI (<https://www.ncbi.nlm.nih.gov/tools/primer-blast>). PCR reactions were conducted using GoTaq G2 Flexi DNA Polymerase (Promega, M7801) as described in Table S4 and Figure S3 (Supporting Information). The PCR products amplified using oligonucleotides P1 and P4, for each target gene (COSMC, MGAT1 and Gal3), were purified from agarose gel using NucleoSpin Gel and PCR Clean-up (MACHEREY NAGEL, 740609) and cloned into linearized vector pCR2.1 using the T4 DNA ligase (both included in the TA cloning kit, ThermoFisher, K202020). Ligation products were then transformed into Stellar competent cells (Takara, 636766). The colonies were allowed to grow overnight at 37 °C on Petri dishes containing LB Agar with 100 µg mL<sup>-1</sup> ampicillin and 50 µg mL<sup>-1</sup> X-Gal for white/blue screening. White colonies were then amplified in LB Broth suspension culture media (overnight incubation, 37 °C, 220 RPM orbital agitation). The resulting plasmids were extracted using Nu-

cleoSpin Plasmid (MACHEREY NAGEL, 740588) and the presence of the insert was checked by digestion using EcoRI (Promega, R6011). Plasmids containing the desired inserts were sequenced by Genewiz/Azenta using M13R universal primers.

**Cell Lines and Viruses:** The human colorectal cell lines, HCT116 (ATCC-CCL-247) and SW620 (ATCC-CCL-227), the triple-negative breast carcinoma cell line MDA-MB-231 (provided by Dr Patrick Legembre, Rennes, France) and the embryonic kidney cell line HEK293T (ATCC-CRL-3216), as well as isogenic cell derivatives, were cultured in DMEM High Glucose medium (Dutscher, L0140-500), supplemented with 10% fetal calf serum (Dutscher). The BT-20 (ATCC-HTB-19) and mouse 4T1 (ATCC-CRL-2539) human and mouse breast cancer cell lines and derivatives, respectively, were cultured in MEM medium with GlutaMAX Supplement (ThermoFisher, 41090028), and RPMI 1640 medium (Dutscher, L0500-500), supplemented with 10% fetal calf serum. Lentiviruses were produced using Lenti-X cells (Takara #632180) that were cotransfected with 11 µg psPAX2 (Addgene # 12260), 3 µg pMD2.G (Addgene # 12259) and 10 µg Lentiviral plasmid using PEI reagent (Merk, 43896) as described by Longo et al.<sup>[53]</sup> Following an overnight incubation, the transfected cells were stimulated with 10 mM sodium butyrate for 8 h to increase the viral production, the media was changed and collected after 16 to 24 h. Prior to infection, target cells were seeded to reach 50 to 60% confluence. Viral supernatants were recovered and filtered using a 0.45 µm sterile filter. 3 mL filtered supernatants, containing 8 µg mL<sup>-1</sup> polybrene were added to the target cells and transduction was favored via spinoculation at 800 × g for 1 h at 30 °C. A total of four round spinoculations were performed. When needed, cells were grown in the presence or absence of antibiotics (puromycin (2.5 µg mL<sup>-1</sup>) or blasticidin (10 µg mL<sup>-1</sup>)) from ThermoFisher.

**Transfection and Enrichment of CRISPR-Cas9-Induced Deficient Polyclonal Cells:** HEK293T and HCT116 cells were transfected using PEI. The PEI reagent was prepared by solubilizing polyethyleneimine, linear, M.W. 25 kDa (Merk, 43896) in deionized water at 80 °C. The solution was allowed to cool down at room temperature and pH was neutralized to 7.0 before sterilization using 0.22 µm filters and stored at -20 °C. The cells were first seeded to reach 80% confluency at the day of transfection. For transfection, plasmid-PEI complexes were prepared at mass ratio of 1:2 (plasmid DNA:PEI) in Opti-MEM Reduced Serum Medium, supplemented with GlutaMAX (ThermoFisher, 51985026). The volume of Opti-MEM used varied according to the dimension of the cell culture dishes used for transfection and represented 10 to 20% of the final volume of the cultured dish. After vortexing, the transfection mix was incubated at room temperature for 15 min and added drop-by-drop to the cells. The culture media was replaced after overnight incubation at 37 °C and 5% CO<sub>2</sub>. 4T1, BT20, MDA-MB-231 and SW620 cells were transfected with LipoFectMax 3000 Transfection Reagent (ABP Biosciences, FP319). The transfection mix was prepared according to manufacturer's protocol and added to empty wells, prior to seeding of the cells. After 24 or 48 h, transfected cells are either enriched by selection using puromycin at a concentration of 1 to 2.5 µg mL<sup>-1</sup> for an additional 48 h or sorted by flow cytometry on FACSMelody (BD Biosciences), under sterile conditions, based on the brightest top 30% EGFP positive cells (unless indicated otherwise). For FACS enrichment of polyclonal cells, the cells were stained with Fixable Viability Stain 660 (BD Biosciences, 564405) in PBS to avoid selection of dead cells (FVS660 positive), resuspended in BD FACS Pre-Sort Buffer (BD Biosciences, 563503), and then recovered in PBS1X, 20 × 10<sup>-3</sup> M HEPES (ThermoFisher, 15630056) containing 10% FBS. After sorting, EGFP positive cells were grown in the usual culture media. For clonal cell sorting, single cells were directly recovered, individually into 96 well plates, as above using single cell precision mask. All flow cytometry experiments were conducted in the core facility ImaFlow (Université de Bourgogne, Dijon).

**Production of Recombinant TRAIL and Fas Ligand:** TRAIL was produced in the BL21 Star (DE3) pLysS *Escherichia coli* strain cell line as described by Schneider.<sup>[54]</sup> Briefly, cells were transformed with pET100D-V2-TRAIL-Mu3 and plated on an agarose plate containing 100 µg mL<sup>-1</sup> ampicillin and 30 µg mL<sup>-1</sup> chloramphenicol. An individual clone was grown overnight in suspension in LB Broth as above (incubation, 37 °C, 220 RPM orbital agitation). The next day the suspension was further amplified in a larger

volume (500 mL) until the OD reached 0.3–0.5 and  $100 \times 10^6$  M IPTG was added to induce the production of the ligand overnight at room temperature. The cell pellet was next recovered by centrifugation ( $5,000 \times g$ , 10 min, 4 °C), resuspended in lysis buffer ( $50 \times 10^{-3}$  M  $\text{NaH}_2\text{PO}_4$ ,  $300 \times 10^{-3}$  M NaCl,  $10 \times 10^{-3}$  M imidazol,  $10 \times 10^{-3}$  M beta-mercaptoethanol, pH 8.0) and frozen and thawed 3 times before clarification by centrifugation ( $16\,000 \times g$ , 30 min, 4 °C). The cleared sample was next filtrated using a 0.45  $\mu\text{m}$  syringe filter and the recombinant protein was purified using Ni-NTA resin (ThermoFisher, 88222) as recommended by the provider, using the native condition protocol.

Fas ligand was produced in MDA-MB-231 Fas KO cells. Briefly, cells were transduced with pAIPACRP30-FasL. The highest expressing cell clone was further amplified for the production of the ligand in the presence of DMEM. Debris was discarded by centrifugation ( $1000 \times g$ , 5 min, 4 °C) and filtration (0.22  $\mu\text{m}$ ) and the recovered conditioned media was stored at -20 °C.

**Treatments and Analysis of Apoptosis:** Cells were stimulated or not with TRAIL-Mu3 ( $2.5 \times 10^{-9}$  M) or Fas ligand (25% of culture media volume) produced as previously described,<sup>[54,55]</sup> and apoptosis was quantified either using the live cell imaging system Incucyte S3 microscope or by flow cytometry after staining with FITC Annexin-V (BioLegend, 640945; according to manufacturer recommendation for flow cytometry and at final dilution of 1/500 for live cell imaging with Incucyte S3), with or without 7AAD (BD Biosciences, 559925) or propidium iodide (Merck, P4170; at final concentration of 2.5  $\mu\text{g mL}^{-1}$ ). Flow cytometry experiments were conducted on BD LSRFortessa Cell Analyzer (BD Biosciences).

**Analysis of TRAIL Receptors, Fas Expression or Cell-Surface Glycans by Flow Cytometry:** Cell surface receptors or glycans staining was performed on nonpermeabilized cells. For receptor staining, cells were saturated for 30 min at 4 °C with a PBS-B solution containing 3% BSA in PBSTX and stained for 60 min on ice with the primary antibodies in PBS-B (1  $\mu\text{g per } 10^6$  cell; anti-DR4, anti-DR5 and anti-Fas). The cells were then washed in ice cold PBSTX and stained with a secondary antibody (Rabbit anti-Mouse IgG (H+L) Alexa Fluor 680; ThermoFisher, A-21065) for 30 min on ice. Staining of glycans was performed on nonpermeabilized cells too as above using the staining buffer lectins solution or SBL ( $30 \times 10^{-3}$  M HEPES,  $10 \times 10^{-3}$  M glucose,  $110 \times 10^{-3}$  M NaCl,  $10 \times 10^{-3}$  M KCl,  $1 \times 10^{-3}$  M  $\text{MgCl}_2$ ,  $1.5 \times 10^{-3}$  M  $\text{CaCl}_2$ , pH 7.2) and biotinylated or Alexa Fluor488 conjugated lectins in SBL (5  $\mu\text{g to } 10 \mu\text{g per } 10^6$  cells; PHA-LAF488 or biotinylated VVL). The cells were then washed in ice cold SBL and stained, when needed with a streptavidin-Alexa Fluor 680 (ThermoFisher, S21378) for 30 minutes on ice. For both staining the cells were then washed 3 times before analysis by flow cytometry using the BD LSRFortessa Cell Analyzer (BD Biosciences).

**Western Blotting:** After stimulation or not, cells (both supernatant and adherent cells) were harvested after trypsinization and centrifugation at  $300 \times g$  for 5 min at 4 °C. Washed once with ice cold PBSTX, cell pellets were lysed in 3 times their estimated volume, using RIPA lysis buffer ( $50 \times 10^{-3}$  M Tris HCl, pH 8.0,  $150 \times 10^{-3}$  M NaCl, 1% Triton-X100, 0.5% sodium deoxycholate, 0.1% SDS) supplemented with Halt Protease Inhibitor Cocktail (100X) and EDTA (ThermoFisher, 78429). 20 mins after incubation on ice, the lysates were centrifuged at  $18\,000 g$  for 18 min at 4 °C to remove cell debris and transferred to a fresh tube, and proteins (25–50  $\mu\text{g}$ ) were loaded and separated by SDS-PAGE then transferred to nitrocellulose membranes. To block nonspecific binding sites, membranes were incubated in 5% skimmed milk for 1h and then washed 3 times with PBS containing 0.5% Tween 20 (PBS-T). Immunoblots were incubated overnight with a specific primary antibody (see Table S3, Supporting Information), washed 3 times in PBS-T then incubated for 1h with the corresponding HRP-conjugated secondary antibody.

Blots were developed using the Covalig Xtra ECL enhanced chemiluminescence reagent (Covalab, 00118075) according to the manufacturer's protocol.

## Supporting Information

Supporting Information is available from the Wiley Online Library or from the author.

## Acknowledgements

Monoclonal antibodies targeting DR4 and DR5 used for flow cytometry were kindly provided by Covalab. The authors thank Pr Pascal Schneider (Lausanne) for the ACRP30-FasL cDNA. O.M. was supported by grants from CCIR Est (Conférence de Coordination Interrégionale Est de la ligue contre le cancer, comité de Côte d'or), the ANR (Agence Nationale de la Recherche) program, "Investissements d'Avenir" Labcom IAM-IT (ANR-22-LCV1-0005-01), Labex LipSTIC (ANR-11LABX-0021-01), ISITE-BFC (ANR-15-IDEX-0003) and the European Union's Horizon 2020 research and innovation program under the Marie Skłodowska-Curie grant agreement No. 777995 (DISCOVER). A.R. was supported by a fellowship from the ANR ISITE-BFC (ANR-15-IDEX-0003) and (ANR-22-LCV1-0005-01).

## Conflict of Interest

The authors declare no conflict of interest.

## Author Contributions

A.R. performed all experiments unless otherwise mentioned; C.J. generated the LRP1 KO cells; M.E. the HSP KO; A.A.C. the C8 lentiviral KO; S.H. generated the TALEN DR5; B.P. produced the Mgat1/COSMC clones; N.P. performed cell sorting; A.G. prepared the Caspase-8 and FADD gRNAs. J.D. supervised the LRP1 KO. O.M. and A.R. analyzed and processed the data. O.M. designed the study. O.M. and A.R. wrote the manuscript.

## Data Availability Statement

The data that support the findings of this study are available in the Supporting Information of this article.

## Keywords

cell sorting, CRISPR/Cas9, gene editing, guide RNA, intracellular gene products, polyclonal cells, puromycin selection

Received: January 17, 2023

Revised: April 11, 2023

Published online:

- [1] E. Deltcheva, K. Chylinski, C. M. Sharma, K. Gonzales, Y. Chao, Z. A. Pirzada, M. R. Eckert, J. Vogel, E. Charpentier, *Nature* **2011**, 471, 602.
- [2] M. Adli, *Nat. Commun.* **2018**, 9, 1911.
- [3] Y. Yang, J. Xu, S. Ge, L. Lai, *Front. Med.* **2021**, 8, 649896.
- [4] K. Saha, E. J. Sontheimer, P. J. Brooks, M. R. Dwinell, C. A. Gersbach, D. R. Liu, S. A. Murray, S. Q. Tsai, R. C. Wilson, D. G. Anderson, A. Asokan, J. F. Banfield, K. S. Bankiewicz, G. Bao, J. W. M. Bulte, N. Bursac, J. M. Campbell, D. F. Carlson, E. L. Chaikof, Z. Y. Chen, R. H. Cheng, K. J. Clark, D. T. Curiel, J. E. Dahlman, B. E. Deverman, M. E. Dickinson, J. A. Doudna, S. C. Ekker, M. E. Emborg, G. Feng, *Nature* **2021**, 592, 195.
- [5] J. W. Woo, J. Kim, S. I. Kwon, C. Corvalan, S. W. Cho, H. Kim, S. G. Kim, S. T. Kim, S. Choe, J. S. Kim, *Nat. Biotechnol.* **2015**, 33, 1162.
- [6] S. A. Oh, A. Seki, S. Rutz, *Curr. Protoc. Immunol.* **2019**, 124, e69.
- [7] A. Seki, S. Rutz, *J. Exp. Med.* **2018**, 215, 985.
- [8] F. Dufour, T. Rattier, A. A. Constantinescu, L. Zischler, A. Morle, H. Ben Mabrouk, E. Humblin, G. Jacquemin, E. Szegezdi, F. Delacote, N. Marrakchi, G. Guichard, C. Pellat-Deceunynck, P. Vacher, P. Legembre, C. Garrido, O. Mischeau, *Oncotargets Ther.* **2017a**, 8, 9974.
- [9] R. H. Smith, Y. C. Chen, F. Seifuddin, D. Hupalo, C. Alba, R. Reger, X. Tian, D. Araki, C. L. Dalgard, R. W. Childs, M. Pirooznia, A. Larochelle, *Genes* **2020**, 11.

- [10] C. J. Giuliano, A. Lin, V. Girish, J. M. Sheltzer, *Curr. Protoc. Mol. Biol.* **2019**, 128, e100.
- [11] C. Liesche, L. Venkatraman, S. Aschenbrenner, S. Grosse, D. Grimm, R. Eils, J. Beaudouin, *BMC Biotechnol.* **2016**, 16, 17.
- [12] Y. Shamshirgaran, A. Jonebring, A. Svensson, I. Leeft, Y. M. Bohlooly, M. Firth, K. J. Woollard, A. Hofherr, I. M. Rogers, R. Hicks, *Sci. Rep.* **2021**, 11, 16532.
- [13] N. E. Sanjana, O. Shalem, F. Zhang, *Nat. Methods* **2014**, 11, 783.
- [14] O. Shalem, N. E. Sanjana, E. Hartenian, X. Shi, D. A. Scott, T. Mikkelsen, D. Heckl, B. L. Ebert, D. E. Root, J. G. Doench, F. Zhang, *Science* **2014**, 343, 84.
- [15] G. Stolfa, N. Mondal, Y. Zhu, X. Yu, A. Buffone Jr, S. Neelamegham, *Sci. Rep.* **2016**, 6, 30392.
- [16] J. Jia, Y. P. Abudu, A. Claude-Taupin, Y. Gu, S. Kumar, S. W. Choi, R. Peters, M. H. Mudd, L. Allers, M. Salemi, B. Phinney, T. Johansen, V. Deretic, *Mol. Cell* **2018**, 70, 120.
- [17] F. Dufour, T. Rattier, S. Shirley, G. Picarda, A. A. Constantinescu, A. Morle, A. B. Zakaria, G. Marcion, S. Causse, E. Szegezdi, D. M. Zajonc, R. Seigneuric, G. Guichard, T. Gharbi, F. Picaud, G. Herlem, C. Garrido, P. Schneider, C. A. Benedict, O. Micheau, *Cell Death Differ.* **2017**, 24, 500.
- [18] O. Micheau, in *TRAIL, Fas Ligand, TNF and TLR3 in Cancer* (Ed: O. Micheau), Springer International Publishing, Cham, Switzerland **2017**, pp. 247–290.
- [19] G. de Vreede, H. A. Morrison, A. M. Houser, R. M. Boileau, D. Andersen, J. Colombani, D. Bilder, *Dev. Cell* **2018**, 45, 595.e4.
- [20] O. M. Shatnyeva, A. V. Kubarenko, C. E. Weber, A. Pappa, R. SchwartzAlbiez, A. N. Weber, P. H. Krammer, I. N. Lavrik, *PLoS One* **2011**, 6, e19927.
- [21] K. W. Wagner, E. A. Punnoose, T. Januario, D. A. Lawrence, R. M. Pitti, K. Lancaster, D. Lee, M. Goetz, S. F. Yee, K. Totpal, L. Huw, V. Katta, G. Cavet, S. G. Hymowitz, L. Amler, A. Ashkenazi, *Nat. Med.* **2007**, 13, 1070.
- [22] J. P. Concordet, M. Haeussler, *Nucleic Acids Res.* **2018**, 46, W242W245.
- [23] J. L. Bodmer, N. Holler, S. Reynard, P. Vinciguerra, P. Schneider, P. Juo, J. Blenis, J. Tschopp, *Nat. Cell Biol.* **2000**, 2, 241.
- [24] M. P. Boldin, T. M. Goncharov, Y. V. Goltsev, D. Wallach, *Cell* **1996**, 85, 803.
- [25] A. T. Ting, F. X. Pimentel-Muinos, B. Seed, *EMBO J.* **1996**, 15, 6189.
- [26] P. Juo, C. J. Kuo, J. Yuan, J. Blenis, *Curr. Biol.* **1998**, 8, 1001.
- [27] G. Kesavan, *Mol. Biotechnol.* **2023**, 65, 38.
- [28] H. Mollanoori, Y. Rahmati, B. Hassani, M. Havasi Mehr, S. Teimourian, *Genes Dis.* **2021**, 8, 146.
- [29] P. Patsali, G. Turchiano, P. Papisavva, M. Romito, C. C. Loucari, C. Stephanou, S. Christou, M. Sitarou, C. Mussolino, T. I. Cornu, M. N. Antoniou, C. W. Lederer, T. Cathomen, M. Kleanthous, *Haematologica* **2019**, 104, e497e501.
- [30] Y. T. Tsai, B. L. da Costa, N. D. Nolan, S. M. Caruso, L. A. Jenny, S. R. Levi, S. H. Tsang, P. M. J. Quinn, *Methods Mol. Biol.* **2023**, 2560, 313.
- [31] S. Demirci, A. Leonard, K. Essawi, J. F. Tisdale, *Mol. Ther. –Methods Clin. Dev.* **2021**, 23, 276.
- [32] A. Pinhas, D. B. Zhou, O. Otero-Marquez, M. V. Castanos Toral, J. V. Migacz, J. Glassberg, R. B. Rosen, T. Y. P. Chui, *Case Rep. Hematol.* **2022**, 2022, 6079631.
- [33] Y. Hu, Y. Zhou, M. Zhang, W. Ge, Y. Li, L. Yang, G. Wei, L. Han, H. Wang, S. Yu, Y. Chen, Y. Wang, X. He, X. Zhang, M. Gao, J. Yang, X. Li, J. Ren, H. Huang, *Clin. Cancer Res.* **2021**, 27, 2764.
- [34] S. F. Lacey, J. A. Fraietta, *Trends Mol. Med.* **2020**, 26, 713.
- [35] Y. Lu, J. Xue, T. Deng, X. Zhou, K. Yu, L. Deng, M. Huang, X. Yi, M. Liang, Y. Wang, H. Shen, R. Tong, W. Wang, L. Li, J. Song, J. Li, X. Su, Z. Ding, Y. Gong, J. Zhu, Y. Wang, B. Zou, Y. Zhang, Y. Li, L. Zhou, Y. Liu, M. Yu, Y. Wang, X. Zhang, L. Yin, *Nat. Med.* **2020**, 26, 732.
- [36] M. Naeimi Kararoudi, S. Likhite, E. Elmas, K. Yamamoto, M. Schwartz, K. Sorathia, M. de Souza Fernandes Pereira, Y. Sezgin, R. D. Devine, J. M. Lyberger, G. K. Behbehani, N. Chakravarti, B. S. Moriarity, K. Meyer, D. A. Lee, *Cell Rep. Methods* **2022**, 2, 100236.
- [37] J. Ren, X. Zhang, X. Liu, C. Fang, S. Jiang, C. H. June, Y. Zhao, *Oncotargets Ther.* **2017**, 8, 17002.
- [38] M. Y. Kim, K. R. Yu, S. S. Kenderian, M. Ruella, S. Chen, T. H. Shin, A. A. Aljanahi, D. Schreeder, M. Klichinsky, O. Shestova, M. S. Kozlowski, K. D. Cummins, X. Shan, M. Shestov, A. Bagg, J. J. D. Morrisette, P. Sekhri, C. R. Lazzarotto, K. R. Calvo, D. B. Kuhns, R. E. Donahue, G. K. Behbehani, S. Q. Tsai, C. E. Dunbar, S. Gill, *Cell* **2018**, 173, 1439.e19.
- [39] S. W. Wang, C. Gao, Y. M. Zheng, L. Yi, J. C. Lu, X. Y. Huang, J. B. Cai, P. F. Zhang, Y. H. Cui, A. W. Ke, *Mol. Cancer* **2022**, 21, 57.
- [40] C. Baum, O. Kustikova, U. Modlich, Z. Li, B. Fehse, *Hum. Gene Ther.* **2006**, 17, 253.
- [41] S. Bijlani, K. M. Pang, V. Sivanandam, A. Singh, S. Chatterjee, *Front. Genome Ed.* **2021**, 3, 799722.
- [42] C. E. Nelson, Y. Wu, M. P. Gemberling, M. L. Oliver, M. A. Waller, J. D. Bohning, J. N. Robinson-Hamm, K. Bulaklak, R. M. Castellanos Rivera, J. H. Collier, A. Asokan, C. A. Gersbach, *Nat. Med.* **2019**, 25, 427.
- [43] K. S. Hanlon, B. P. Kleinstiver, S. P. Garcia, M. P. Zaborowski, A. Volak, S. E. Spirig, A. Muller, A. A. Sousa, S. Q. Tsai, N. E. Bengtsson, C. Loov, M. Ingelsson, J. S. Chamberlain, D. P. Corey, M. J. Aryee, J. K. Joung, X. O. Breakefield, C. A. Maguire, B. Gyorgy, *Nat. Commun.* **2019**, 10, 4439.
- [44] N. Holler, R. Zaru, O. Micheau, M. Thome, A. Attinger, S. Valitutti, J. L. Bodmer, P. Schneider, B. Seed, J. Tschopp, *Nat. Immunol.* **2000**, 1, 489.
- [45] F. C. Kischkel, D. A. Lawrence, A. Chuntharapai, P. Schow, K. J. Kim, A. Ashkenazi, *Immunity* **2000**, 12, 611.
- [46] O. Micheau, *Int. J. Mol. Sci.* **2018**, 19, 715.
- [47] S. C. Sleight, B. A. Bartley, J. A. Lieviant, H. M. Sauro, *Nucleic Acids Res.* **2010**, 38, 2624.
- [48] A. A. Gooden, C. N. Evans, T. P. Sheets, M. E. Clapp, R. Chari, *Nucleic Acids Res.* **2021**, 49, D871.
- [49] N. Holler, A. Tardivel, M. Kovacovics-Bankowski, S. Hertig, O. Gaide, F. Martinon, A. Tinel, D. Deperthes, S. Calderara, T. Schulthess, J. Engel, P. Schneider, J. Tschopp, *Mol. Cell. Biol.* **2003**, 23, 1428.
- [50] H. Zhu, J. Yan, Q. Xu, L. Wei, X. Huang, S. Chen, C. Yi, *Mol. Med. Rep.* **2017**, 16, 9607.
- [51] P. J. Shilling, D. O. Daley, *Bio-Protoc.* **2021**, 11, e4133.
- [52] P. J. Shilling, K. Mirzadeh, A. J. Cumming, M. Widesheim, Z. Kock, D. O. Daley, *Commun. Biol.* **2020**, 3, 214.
- [53] P. A. Longo, J. M. Kavran, M. S. Kim, D. J. Leahy, *Methods Enzymol.* **2013**, 529, 227.
- [54] P. Schneider, *Methods Enzymol.* **2000**, 322, 325.
- [55] M. Huang, C. Yi, X. Z. Huang, J. Yan, L. J. Wei, W. J. Tang, S. C. Chen, Y. Huang, *Oncol. Lett.* **2021**, 21, 438.